Journal of Cluster Science (2020) 31:1349–1362
https://doi.org/10.1007/s10876-019-01746-x

ORIGINAL PAPER

Bioactive Wound Dressing Gauze Loaded with Silver Nanoparticles Mediated by Acacia Gum

Mehrez E. El-Naggar[1] · Abdelrahman M. Abdelgawad[1,3] · Dalia A. Elsherbiny[2,3] · Waffa A. El-shazly[2] · Samaneh Ghazanfari[3] · Mohamed S. Abdel-Aziz[4] · Yasser K. Abd-Elmoneam[2]

Received: 16 November 2019 / Published online: 9 December 2019

Abstract

A wound dressing is very crucial component in wound healing process. Bioactive dressings play important role in wound sterilization and promote tissue healing and growth. The present work investigated the preparation of AgNPs in solid-state using acacia gum as both reductant and stabilizing agent. Sodium hydroxide (NaOH) was employed as activating agent and pH mediator. Acacia is a naturally occurring mixture of polysaccharides and glycoproteins. The obtained particles were in the range of 50 nm. The work was extended to evaluate the antimicrobial of AgNPs treated gauze cotton fabrics against gram positive (*S. aureus*), gram negative (*P. aeruginosa*) bacteria, *C. albicans* (yeast); and *A. Niger* (fungus). The inhibition zone of the as prepared silver nanoparticles was found to be 24 mm against both types of bacteria, 23 mm against *C. albicans* (yeast), and inactive against *A. Niger* (fungus). On the other hand, the treated gauze showed bactericidal behavior and a clear zone was found underneath the samples on the agar plate. The reduction percent in number of bacterial colonies of treated gauze fabrics in comparison to control *Pseudomonas aeruginosa* culture showed a reduction up to 100%. The aforementioned results promote the acquirement of bioactive antibacterial wound dressing.

Keywords Acacia gum · Silver nanoparticles · Solid state · Gauze fabric · Wound dressing

Introduction

Nanotechnology provides new potentials to fight and prevent disease using small and/or atomic sized materials. Metallic nanoparticles show unique chemical activity. This might be attributed to their enormous surface to volume ratios and crystallographic surface [1]. Nanomaterials is considered as a part from nanotechnology science that have active surface area, and very small size [2]. These mentioned parameters encourage the application of nanomaterials in many different applications such as pharmaceutical applications such as anti-cancer, anti-parasite, bactericidal and fungicidal, etc. [3–6].

Among all the candidates applied for the treatment of infections with bacteria, silver nanoparticles (AgNPs) have drawn much attention. AgNPs are capable of considerably broadening the therapeutic efficiency of wound dressings when the later augmented in its structure [7]. Upon the reduction of silver particles to nanoscale dimensions, the antimicrobial properties dramatically increase, however, the characteristic metallic color is not observed. Various preparation routes for (AgNPs) were reported in the literature for instance; reverse micelles method [8], salt reduction [9], reduction using microwave [10], ultrasonic irradiation [11], radiolysis route [12], solvothermal synthesis [13], electrochemical synthesis [14], etc. In the previously mentioned methods the colloidal stability, particle size and the reactivity of the nanoparticles strongly

✉ Mehrez E. El-Naggar
Mehrez_chem@yahoo.com; mehrezeelnaggar@gmail.com

✉ Abdelrahman M. Abdelgawad
aabdelg@ncsu.edu

[1] Textile Research Division, National Research Centre, Dokki, Cairo, Egypt

[2] Chemistry Department, Faculty of Science, Menoufia University, Shebin El-Koom, Menoufia, Egypt

[3] Aachen-Maastricht Institute for Biobased Materials, Faculty of Science and Engineering, Maastricht University, Maastricht, The Netherlands

[4] Genetic Engineering and Biotechnology Division, National Research Center, Dokki, Cairo, Egypt

affected by the synthesis route and the experimental conditions applied.

On the other hand, more eco-friendly synthetic routes have been developed for preparation of metallic nanoparticles via biological sources such as fungi, bacteria, and plant extracts [5, 15–18].

It is worthy to mention that majority of the procedures, which use liquid-state reactions for preparation of AgNPs lack particle stability. The as prepared particles tend to aggregate even at low concentration of the metal salts [19]. Thus, the liquid state synthesis of colloidal AgNPs includes some points of weakness such as; it is important for using strong protecting agents for AgNPs stabilization to prevent the further agglomeration that occur after storing for a long time. Additionally, the high cost for preparation due the utilization of solvents, water, high concentration of reductant and stabilizing agents. The main disadvantage for using the liquid state synthesis is difficulty of scaling up, commercialization and transportation process [19, 20]. Therefore, solid-state synthesis of AgNPs became more popular [19, 21, 22].

Previously, we reported solid-state preparation of silver nanoparticles mediated via soybean protein and cellulose nanocrystals [19, 23]. High nanoparticles content in the final matrix is feasible and reproducible, which simplify management and shipping in the industrial fields. The produced particles tend to have high stability because of the presence of a physical hindrance, which inhibit particles' agglomeration. Additionally, solvents removal from the synthetic medium is cost effective. Many natural polymers such as starch [24], cellulose [23], and soybean protein [19] have been engaged in solid-state synthesis of metal nanoparticles and served as both capping and reducing medium. However, the space is still open for more environmentally benign polymers to be investigated and introduced. According to our initial search, there are no publications or investigations in the literature that reported the use of acacia as medium for AgNPs solid-state preparation.

The basic definition of an injury is any destruction or damage to a living organism that is caused by cuts, hits, accidents, etc. Globally, millions of people are injured for different reasons, for instance, accidents and wars. These injuries range from insignificant to life threatening ones [25]. Wounds are a major type of injuries in which skin and other body tissues broke. Wounds can happen in different format such as scratches, scrapes, cuts, and punctured skin and/or tissues. Minor wounds usually are easier to care; however, they should be cleaned on regular basis to prevent infections. Serious and acute wounds may propagate and get infected easily so that they usually require first aid followed by a visit to emergency rooms [26]. Wound healing process is a physiological course, which includes the group effort of many cell strains as well as their products. The biochemical procedures of wound repair go through phases as following: first, inflammatory reaction takes place; second, cell proliferation and production of the extracellular matrix components; and finally, the posterior remodeling period. These phases happen simultaneously and overlap over time. Therefore, a dressing is very essential component of wound care cycle [27].

The ultimate goal of any wound dressing is to provide a sterile environment, which can promote the granulation and growth of epithelial cells. This clean media will then decrease the threat of infection; however, complete microbial inhibition requires functional dressings [28, 29]. Therefore, dressings are divided to passive and interactive dressings. Passive dressings like gauze and cotton wool are in dictated only for superficial and dry wounds with minimal exudates. On the other hand, interactive dressings such as semi-permeable dressings and hydrogel dressings allow the transport of the fluids in and out [30]. Passive dressings like cotton gauze [31] can be functionalized by the incorporation of antibiotics in order to prevent bacterial infection and expedite the wound healing process. However, the antibiotic resistance of microbes has recently become a global health concern due to perhaps the misuse of existing drugs.

Hereby, the under current work is designed to prepare AgNPs in solid state using acacia gum as reducing and capping stabilizer. A base, NaOH, was applied for Acacia activation and pH mediation. Acacia is mixture of polysaccharides and glycoproteins and it is a main component in many of edible items by humans such as chocolates and soft drinks. Additionally, it has been used as drug carrier to regulate and slow the absorption of amoxicillin in the gut. The as synthesized AgNPs formed at different concentration of $AgNO_3$ were used to finish the cotton gauze to be used as wound healing fabrics. Different characterization techniques such as Uv–vis, ATR-FTIR, TEM, SEM, EDX, DLS, XRD, and particle size analyzer were employed to explore the properties of AgNPs. Furtherly, the antimicrobial properties of AgNPs treated cotton gauze against gram-positive *S. aureus*, gram-negative *P. aeruginosa* bacteria; *C. albicans* (yeast); and *A. Niger* (fungus) were evaluated by recording the zone of inhibition as well as counting the reduction in bacterial cell counts.

Materials and Methods

Materials

Acacia gum as a natural polymer was obtained from Sigma-Aldrich Co. (USA). Silver nitrate ($AgNO_3$) and Sodium hydroxide (NaOH) were of analytical grade and

used without further purification. Bleached gauze fabrics were gifted by El-Mehalla Elkobora Co. for Weaving and Dyeing, Egypt.

Methods

Preparation of Silver Nanoparticles (AgNPs)

Solid-state synthesis of silver nanoparticles (AgNPs) was achieved via acacia gum as an environmentally benign polymer. Acacia polymer acted the dual role of reductant and protecting agent in presence of alkali; sodium hydroxide (NaOH). The synthesis carried out as follow: Acacia gum (0.2 g) was finely grinded followed by the addition of NaOH (0.25 g/1 g acacia gum) and the mixture was mixed mechanically for 5 min in a mortar. Subsequently, different concentrations of silver nitrate ($AgNO_3$) precursor (0.05, 0.10, 0.20 g) was added and the mechanical grinding was continued until the color of solid mixtures solids turned to yellow and blackish yellow depending on the added concentration of $AgNO_3$ proving the formation of AgNPs. Finally, AgNPs samples were calcinated at 110 °C and kept in brown glass bottle for further characterization and application. From our experiment, it was clear that NaOH plays a critical role in activation of acacia molecules and consequently silver ion reduction so that there was no color change in case of its absence.

Cotton Fabrics Treated with Silver Nanoparticles

After full characterization of the obtained AgNPs at different concentrations of the silver salt precursor ($AgNO_3$), the finishing solution was prepared using 0.1 g of $AgNO_3$/1 g Acacia) was selected for fabrics treatment. Different concentrations of the formed AgNPs in its powder form (0.01 g, 0.02 g, 0.04 g, 0.06 g) were suspended in 100 ml of distilled water and kept under contentious magnetic stirrer for 10 min at room temperature. After complete dispersion, each sample of gauze fabrics was immersed in AgNPs colloidal solution for 5 min and squeezed with pick up 100% using pad dry cure technique. The wet samples were dried at 70 °C for 5 min and cured at 120 °C for 2 min.

Characterization

The wavelength of the as synthesized AgNPs prepared at different concentration was monitored using UV–vis spectroscopy (Shimadzu UV-1800; Shimadzu Co., Kyoto, Japan) after diluted 10 times. The particle shape in the solid state was assessed using Transmission Electron Microscopy (JEOL, JEM-1230, Japan, acceleration voltage = 120 kV). The average hydrodynamic particle size and polydispersity index (PDI) of AgNPs were examined using Dynamic light scattering (DLS). For such analysis Zeta sizer nano series (Malvern, UK) was employed to measure the average size as well as the surface charge of the formed particles. Approximately, three cycles of

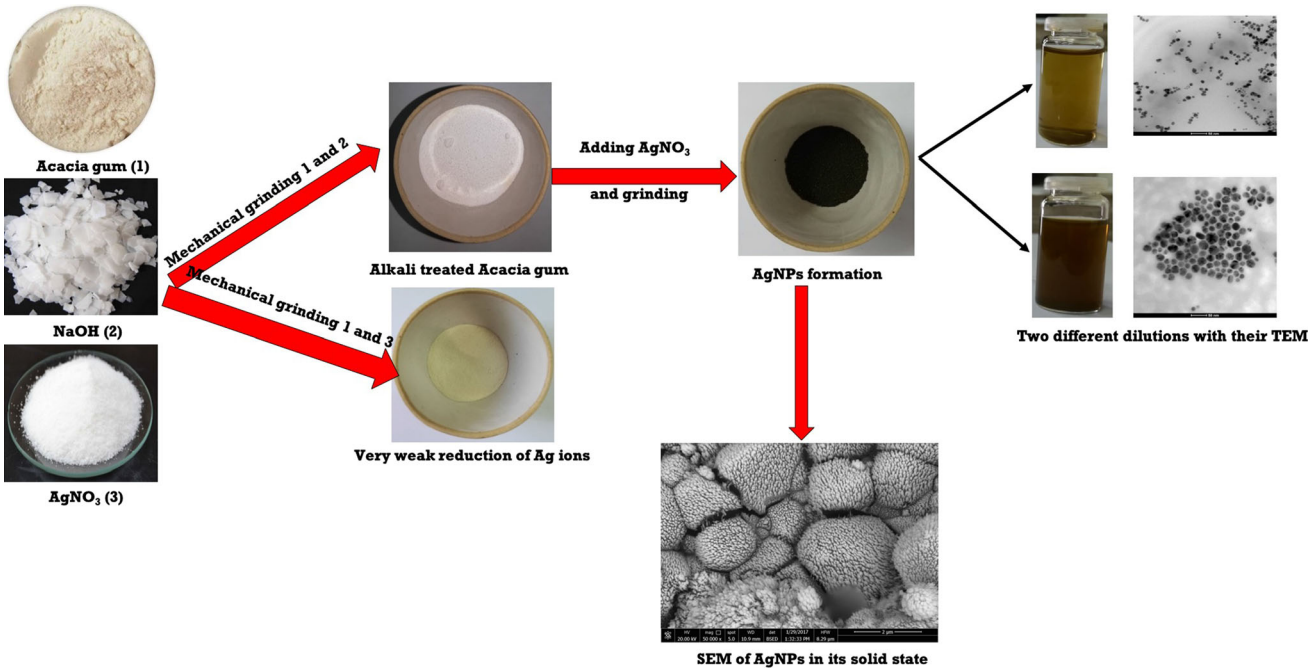

Scheme 1 Solid-state preparation of AgNPs mediated via Acacia gum

Fig. 1 Photographic images of AgNPs powders synthesized at different concentrations of silver nitrate. Where AgNPs-1 = 0.05 g $AgNO_3$/0.2 g Acacia and AgNP-2 = 0.10 $AgNO_3$/0.2 g Acacia and AgNPs-3 = 0.2 g $AgNO_3$/0.2 g Acacia

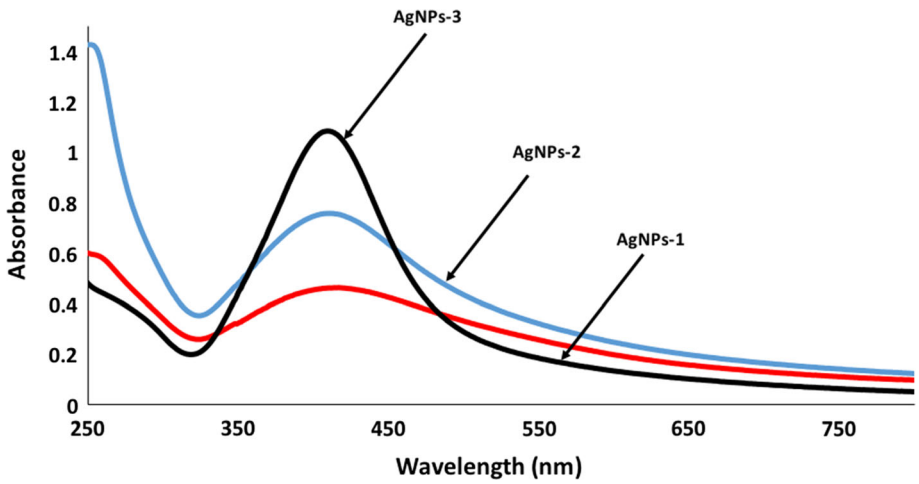

Fig. 2 UV–vis spectra of the AgNPs synthesized at different $AgNO_3$ loads. Where AgNPs-1 = 0.05 g $AgNO_3$/0.2 g Acacia and AgNP-2 = 0.10 $AgNO_3$/0.2 g Acacia and AgNPs-3 = 0.2 g $AgNO_3$/0.2 g Acacia

different counts were tracked and the average of the counts was calculated.

The morphological features and elemental analysis of gauze fabrics before and after AgNPs treatment were investigated using scanning electron microscope connected to energy dispersive X-ray (SEM–EDX; Hitachi S3200, voltage = 20 kV). Samples were mounted on a double-sided carbon tape then coated with a micrometer layer of palladium gold alloy for better imagining.

The characteristic peaks of AgNPs at specific wavenumber (cm^{-1}) were established using FTIR Spectroscopy (Nexus 670; Nicollet, Madison, WI, USA).

Finally, the antimicrobial properties of the as prepared AgNPs powder as well as the treated gauze fabric were assessed against gram positive *S. aureus (*ATCC 6538), gram negative *P. aeruginosa* bacteria ATCC 25416; *C. albicans* ATCC 10231 (yeast); and *A. Niger* NRRL A-326 (fungus).

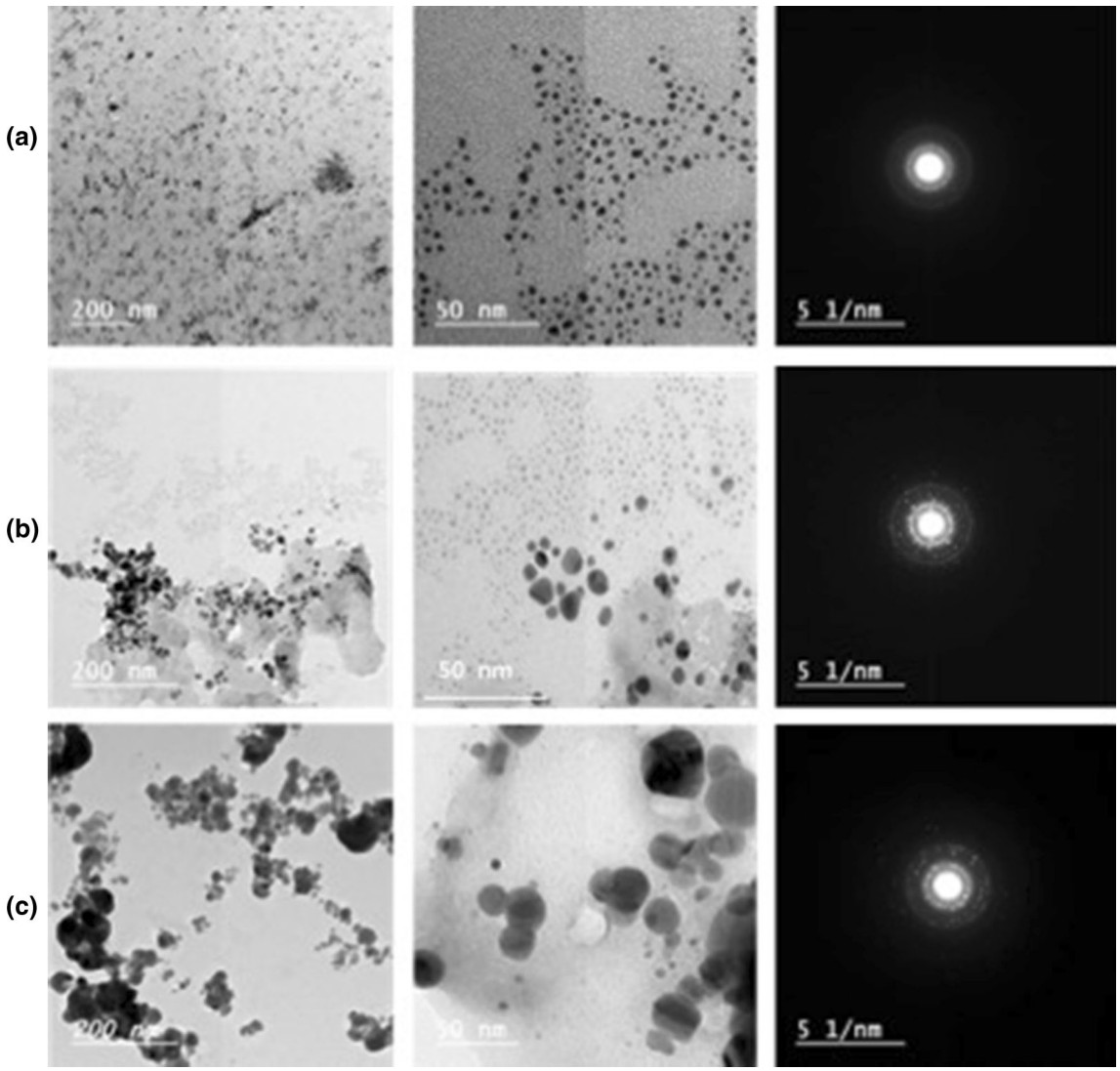

Fig. 3 TEM images and selected area electron diffraction at low and high magnification for AgNPs prepared using different concentrations of $AgNO_3$. Where AgNPs-1 = 0.05 g $AgNO_3$/0.2 g Acacia and AgNP-2 = 0.10 $AgNO_3$/0.2 g Acacia and AgNPs-3 = 0.2 g $AgNO_3$/0.2 g Acacia

The activity was qualitatively tested by the use of disk diffusion method and quantitatively explored via viable cell count method. In the disk diffusion method, the antimicrobial activity is evaluated by measuring sample's inhibition zone on agar plates seeded with microbe species. Samples were placed in small wells of thin agar plates containing rich nutrition medium and approximately 1×10^7 bacterial cells. The plates were incubated overnight at 37 °C then the zones of inhibition were measured.

On the other hand, in viable cell counting method, treated gauze fabrics were kept into contact with the bacterial solution overnight and incubated at 37 °C for 24 h. Specific volume of the supernatant taken out and spread over agar plate, then incubated at 37 °C. The survival bacteria colonies were counted after 24 h. The reduction percentage of bacterial colonies was calculated by the following equation:

$$\boldsymbol{R}(\%) = \left[\frac{(\boldsymbol{A} - \boldsymbol{B})}{\boldsymbol{A}}\right] \times 100$$

where R = the reduction rate, A = the number of bacteria colonies from untreated fabrics, and B = the number of bacteria colonies from treated fabrics.

Results and Discussion

The formation of AgNPs was continuously observed via color change with naked eye. The graphical abstract illustrates the steps for the preparation of AgNPs (Scheme 1). As shown, the color of acacia is white and

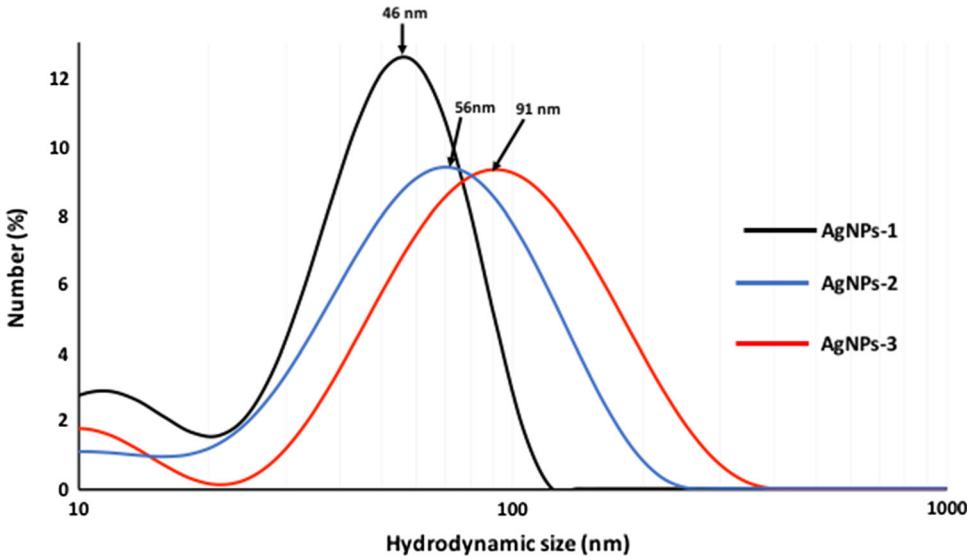

Fig. 4 Particle size analysis of AgNPs synthesized at different concentrations of $AgNO_3$. Where AgNPs-1 = 0.05 g $AgNO_3$/0.2 g Acacia and AgNP-2 = 0.10 $AgNO_3$/0.2 g Acacia and AgNPs-3 = 0.2 g $AgNO_3$/0.2 g Acacia

when grinded with NaOH, it turns to white off. Further mixing with the solid concentration of $AgNO_3$ and submitted to grinding for a certain time, the color converts to yellowish or brownish color depending on the mount of $AgNO_3$ added, which illustrate the formation of AgNPs via the effect of reducing groups located on the backbone of acacia chain.

The reduction activity of acacia gum was improved by the presence of NaOH, which not only offers the favorable basic medium for the reduction reaction, but also swells acacia polymer and expose the bulk active groups on the chains [32]. It is noted that, in the absence of NaOH, the color of acacia does not change even with the addition of high concentration of $AgNO_3$ (data not shown) confirming that NaOH plays an important role in activating acacia molecules to be capable for acting as reducing agent for Ag ions (Fig. 1). For further confirmation the preparation of AgNPs, more advance techniques were used such as TEM, particle size analyzer, zeta potential and SEM–EDX techniques.

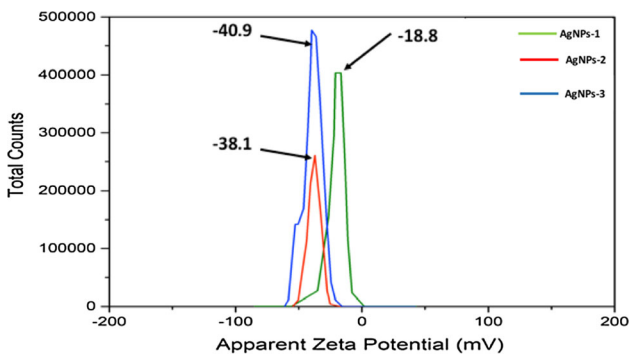

Fig. 5 Zeta potential values of the acacia mediated AgNPs. Where AgNPs-1 = 0.05 g $AgNO_3$/0.2 g Acacia and AgNP-2 = 0.10 $AgNO_3$/0.2 g Acacia and AgNPs-3 = 0.2 g $AgNO_3$/0.2 g Acacia

Firstly, Uv–vis spectrum technique was utilized to determine the absorption peaks for AgNPs (Fig. 2). In our work, we used three different concentrations of $AgNO_3$ (0.05, 0.10 and 0.20 g/0.2 g Acacia) to prepare three different concentrations of AgNPs in their solid state. For analysis, AgNPs colloidal solution was prepared by dispersing a certain weigh of the solid synthesized AgNPs (0.001 g) in a certain volume of distilled water (50 mL). The three analyzed samples were coded depending on the concentration of $AgNO_3$ (0.05, 0.10 and 0.20 g) with AgNPs-1, AgNPs-2 and AgNPs-3 respectively. It is clearly seen that the formed colloidal solution of AgNPs exhibit a typical surface plasmon absorption maxima at 420 nm.

The color change from light yellow to yellowish brown is due to the excitation of surface plasmon vibrations in the formed metal nanoparticles. On the other hand, blank samples without silver ions showed no change in color when prepared under the same conditions. Majority of metals can be treated as free-electron systems and labeled as plasma. This system comprises equivalent numbers of positive ions, fixed in position, and conduction electrons, highly mobile. Upon exposure to electromagnetic wave, the free electrons oscillate coherently by the electric field. These collective oscillations of the free electrons are called plasmons. Consequently, these oscillating plasmons interact with visible light in a phenomenon called surface plasmon resonance (SPR) [15, 33].

Sample coded with AgNPs-1 containes the lowest concentration of silver precursor, $AgNO_3$ and consequently, lower concentration of formed AgNPs. A slight color change from white to pale yellow was visualized suggesting the low conversion of Ag ions to AgNPs. A Uv–vis spectrum of a broad absorption band was obtained, which confirms the low concentration of AgNPs in the sample. Up

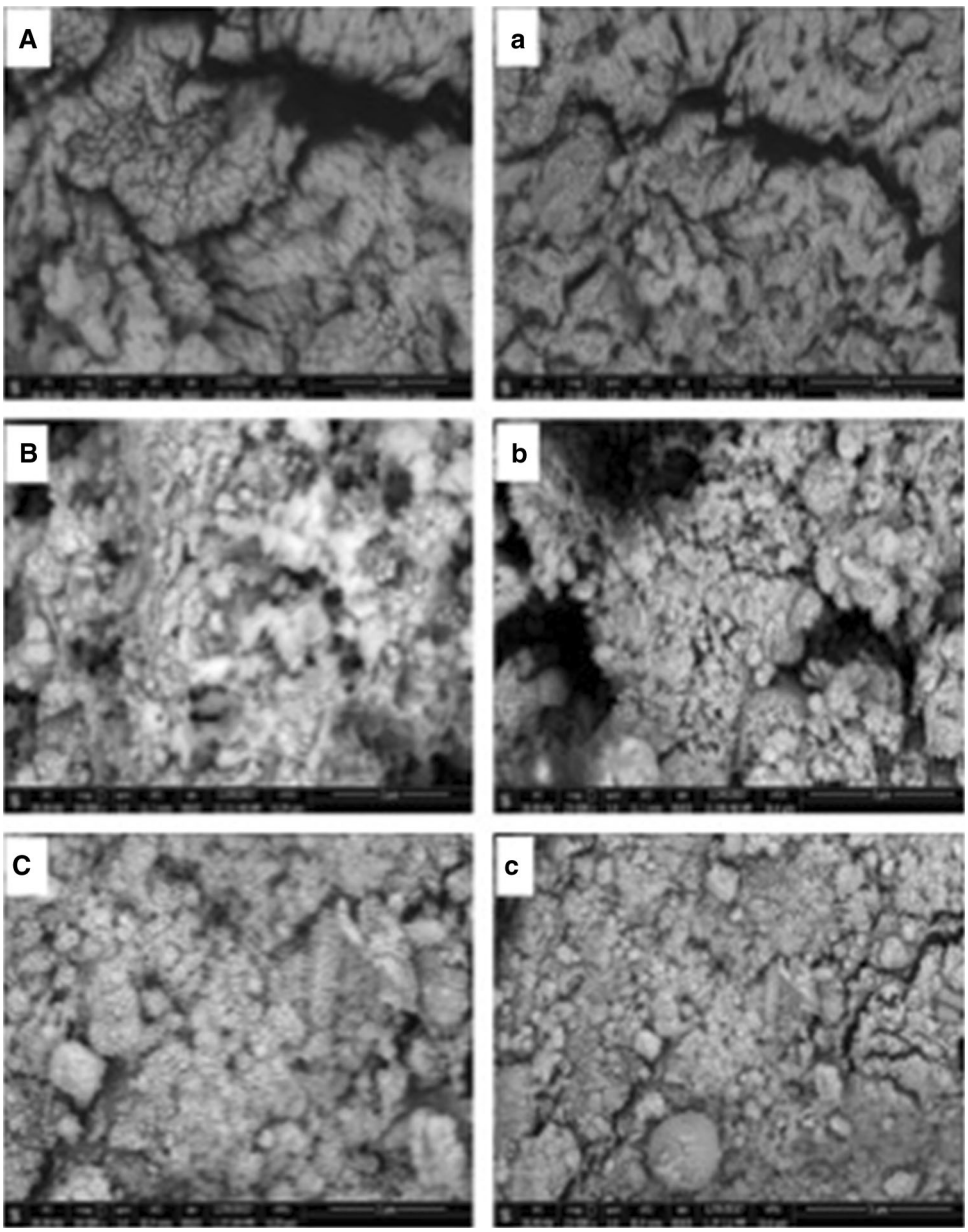

Fig. 6 SEM image of AgNPs with different concentrations examined at low and high magnifications **A**, **a** AgNPs-1 = 0.05 g $AgNO_3$/0.2 g Acacia and **B**, **b** AgNP-2 = 0.10 $AgNO_3$/0.2 g Acacia and **C**, **c** AgNPs-3 = 0.2 g $AgNO_3$/0.2 g Acacia respectively

on increasing silver precursor concentration in the original sample, (0.1 g $AgNO_3$/1 g acacia) as observed for sample (AgNPs-2), the absorption peak becomes sharp indicating that the number of particle size increased. Further increasing the concentration to (0.20 g $AgNO_3$/1 g acacia), the absorption peak become stronger and more symmetrical with a distinct bell shape at a maximum wavelength around 420 nm. The formation of the absorption band is attributed to the phenomenon of surface plasmon resonance excitation that characterize AgNPs.

Figure 3 presents the TEM micrographs and selected area electron diffraction (SAED) of AgNPs at low and high magnifications. Figure 3a shows the shape of AgNPs prepared using the lowest concentration of metal precursor, $AgNO_3$ (0.05 g/1 g acacia). It is clearly observed that the particle shape is spherical with definite edges and very small size confirming that acacia has the competence to reduce and stabilize the formed AgNPs in presence of NaOH. Further increasing the concentration of $AgNO_3$ with fixed amount of acacia (0.1 g/1 g acacia) the particle size marginally increases but less than 20 nm with good distribution (Fig. 3b).

With using 0.2 g of $AgNO_3$ (Fig. 3c) for preparing AgNPs, the particle size increases with less homogeneity and less distribution because of the unavailability of active functional groups in acacia to well-stabilize the formed AgNPs, which consequently leads to the formation of aggregates and particles of large sizes. In addition, SAED

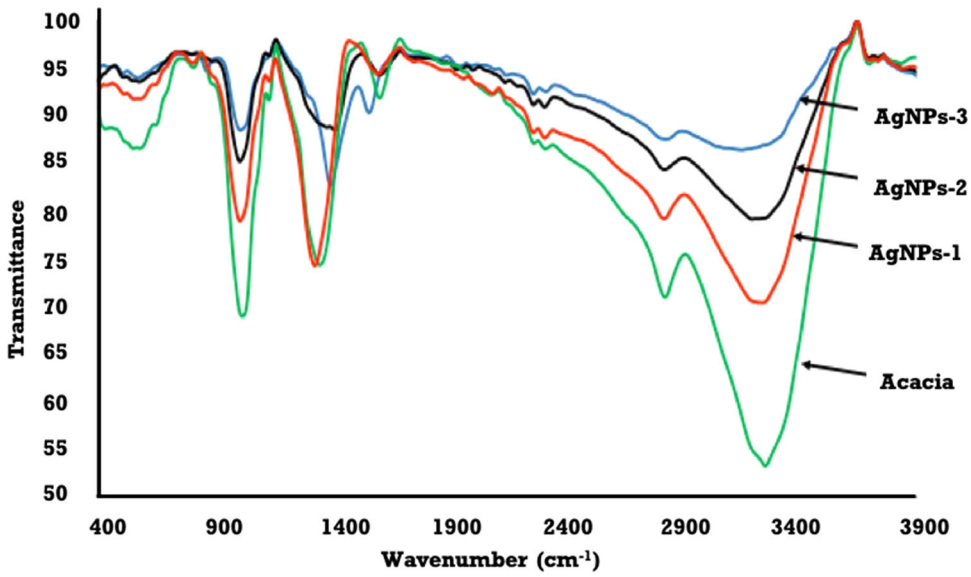

Fig. 7 FTIR spectrum of acacia and AgNPs formed at different silver precursor loadings. Where AgNPs-1 = 0.05 g $AgNO_3$/0.2 g Acacia and AgNP-2 = 0.10 $AgNO_3$/0.2 g Acacia and AgNPs-3 = 0.2 g $AgNO_3$/0.2 g Acacia

of the as synthesized AgNPs at all $AgNO_3$ concentration levels exhibit four planes proving the crystallinity of the nanoparticles. Largely, all the formed AgNPs are still in the nanoform with small size depicting that the method of preparation is efficient and facile to be used in industrial scale without any noticeable drawbacks.

The accurate average size for AgNPs in a colloidal solution was further recorded via dynamic light scattering (DLS) technique. In Fig. 4, the DLS analysis of powdered AgNPs prepared using different concentrations of $AgNO_3$ is shown. The hydrodynamic particle size of AgNPs (AgNPs-1) exhibit average size around 46 nm with PDI (0.05). On the other hand, for the sample coded AgNPs-2, the size increased to 56 nm and sharply increased to 91 nm for the sample labeled with AgNPs-3. The difference in particle sizes of AgNPs might be attributed to the reducing and stabilizing efficacy of acacia gum. At lower concentrations of $AgNO_3$ (AgNPs-1), the availability of the reducing moieties and the stabilizing groups in acacia are obvious and abundant. There are more reducing sugar ends and stabilizing groups are available for the reduction of Ag^+ to Ag^0 and stabilizing the formed Ag^0 clusters, respectively. The accessibility of such active groups would decrease or loss their efficiency with increasing the concentration of $AgNO_3$ (0.1 g and 0.2 g). Therefore, the size increased to 56 nm and 91 nm respectively.

It is also prominent that the size recorded via DLS technique is larger than that of the TEM micrographs, which may be attributed to the swelling effect of AgNPs loaded AgNPs in the measurement solution. To investigate the stability of AgNPs against agglomeration overtime, surface charge (zeta potential) determination is necessity for this purpose. Figure 5 reveals the zeta potential values of AgNPs prepared at different $AgNO_3$ concentrations. It is observed that zeta potential values of AgNPs prepared at 0.05, 0.10 and 0.20 g $AgNO_3$ are − 18.8 mv, − 38 mv and − 40 mv, respectively.

Colloidal solutions with zeta potential values equal or above − 30 mv or + 30 mv exhibit reasonable stability for the particles and thus the particles are being protected against aggregation [34]. Based on this knowledge, the particles prepared from 0.1 and 0.2 g of $AgNO_3$ are more stable. Furthermore, the negative signal is credited to the negatively charged hydroxyl groups located on the backbone of acacia gum. These negative charges inhibit, to large extent, particles' aggregation through electric repulsion force generated between similar neighboring negatively charged molecules. This occurrence of electric repulsion in all probability causes stabilization of particles in their colloidal solutions. Thus, the prominent feature of the AgNPs is the stability; whether synthesized as solid powder or re-dispersed in colloidal solution.

Morphology of Particles: Scanning Electron Microscopy

Figure 6 represents the SEM micrographs for AgNPs prepared using acacia gum as reductant and protecting agent against agglomeration. The figure clearly shows that the surface of native acacia become rougher upon the formation of AgNPs. Furthermore, higher agglomerations are observed as the initial concentration of silver precursor, $AgNO_3$, is increased in the sample.

Fourier Transform Infrared Spectroscopy (FTIR)

The interaction between Acacia and silver salt was studied using FTIR spectroscopy. Figure 7 shows the observed

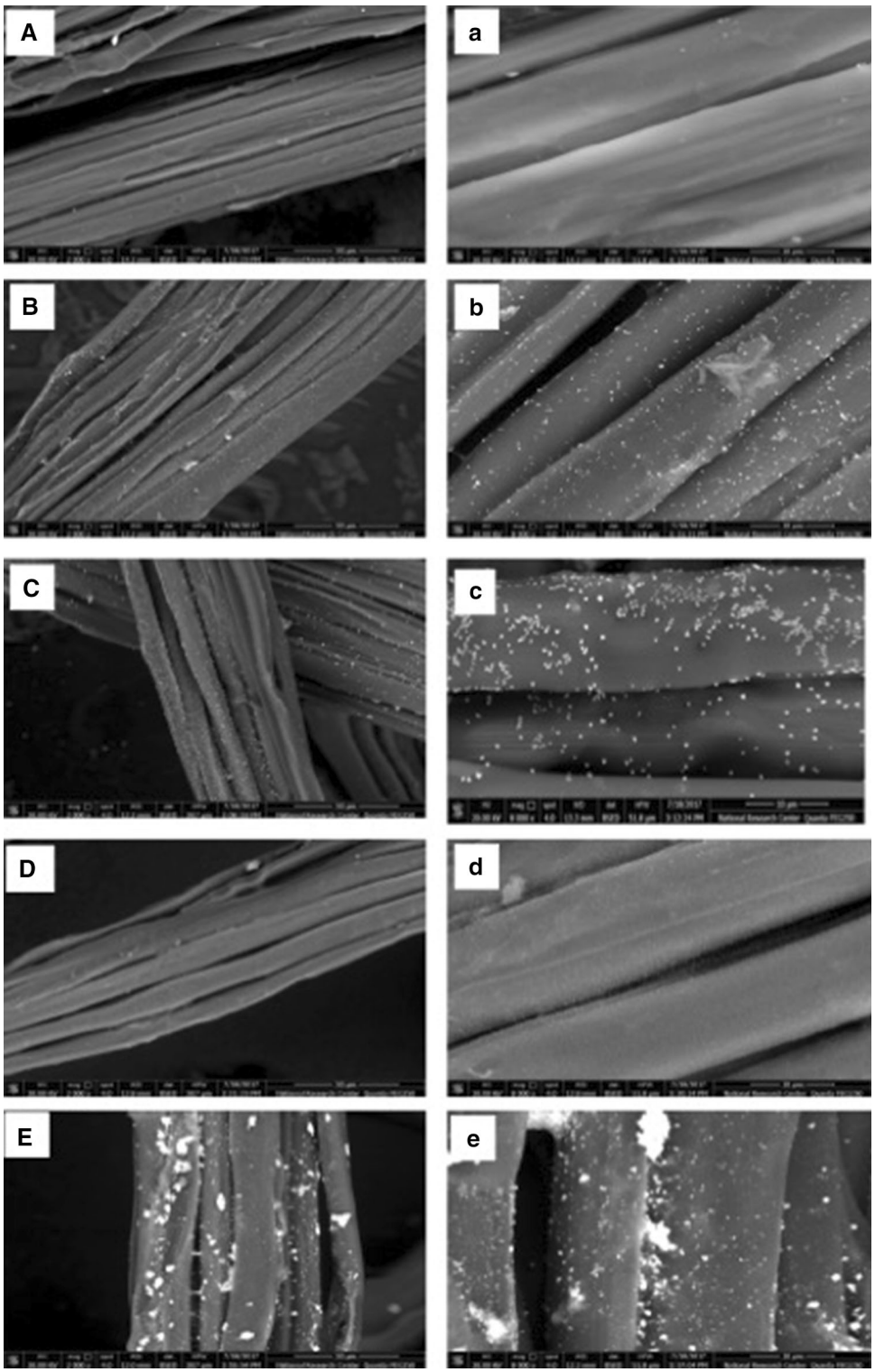

Fig. 8 SEM micrographs of **A**, **a** untreated gauze cotton fabrics and gauze cotton fabrics treated with AgNPs **B**, **b** 0.01 g, **C**, **c** 0.02 g, **D**, **d** 0.04 g, and **E**, **e** 0.06 g

peaks of the untreated acacia spectrum at 3500–3400 cm^{-1}, 2930–2940 cm^{-1} and 1630–1640 cm^{-1} are relevant to O–H stretching, C-H stretching and O-C-H stretching respectively.

On the other hand, the spectra of the treated acacia with three concentrations of $AgNO_3$, (0.05, 0.10 and 0.20 g) coded as (AgNPs-1, AgNPs-2 and AgNPs-3), respectively, show an additional peak at 460–470 cm^{-1} relevant to AgNPs formation. It can also be observed that the intensity of AgNPs peak increased as the concentration of AgNPs increased. The detected peak of OH functional group for the treated acacia showed the lower intensity than the

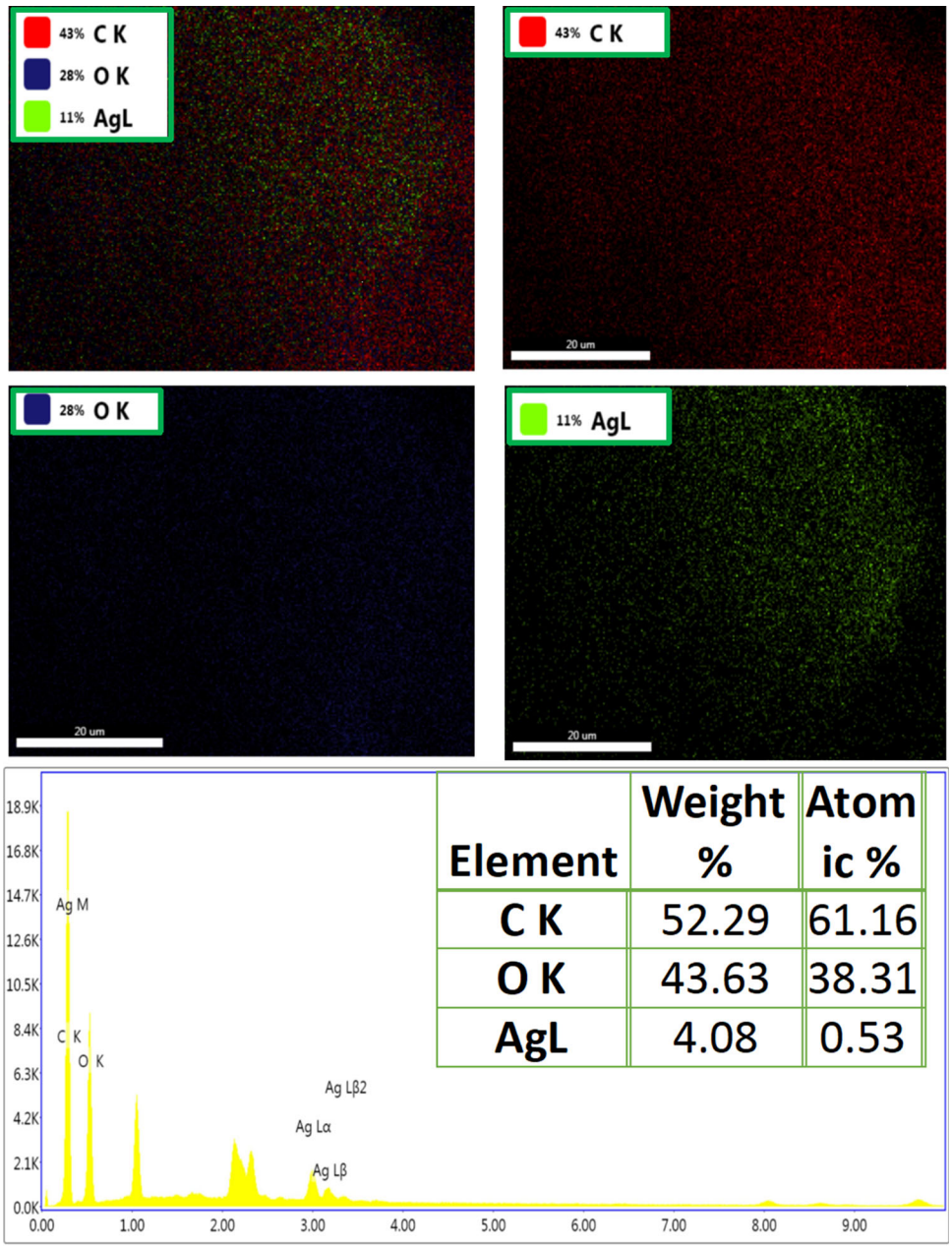

Fig. 9 EDX analysis of gauze fabric treated with AgNPs colloidal solution (0.06/100 mL H_2O)

untreated one. This decrease in peak intensity can be related to the occupation of OH functional group of acacia with AgNPs which in turn cause lower detection by the instrument.

Morphology of Gauze Fabrics Treated with AgNPs using SEM Technique

Colloidal solutions of AgNPs (0.01 g, 0.02 g, 0.04 g, 0.06 g/100 ml H_2O) were prepared. Gauze fabrics were soaked in these solutions then dried at 70 °C for 5 min and cured at 120 °C for 2 min.

Scanning Electron Microscopy (SEM) was employed to investigate the surface features of treated gauze fabrics in comparison with the untreated blank. Figure 8A, a shows the images of untreated cotton fabrics with a smooth surface. Figure 8B–E shows the images of the gauze cotton fabrics after treatments with different concentrations of AgNPs (0.01, 0.02, 0.04 and 0.06 g) respectively. It is obvious that the amount of AgNPs deposited on the fiber surface increases as the concentration of AgNPs colloids solution increases. The images suggest that AgNPs are evenly located on the surface of the gauze fibers. It is worthy to mention that larger agglomerates can be seen on the surface of the fabrics due to the formation of bigger

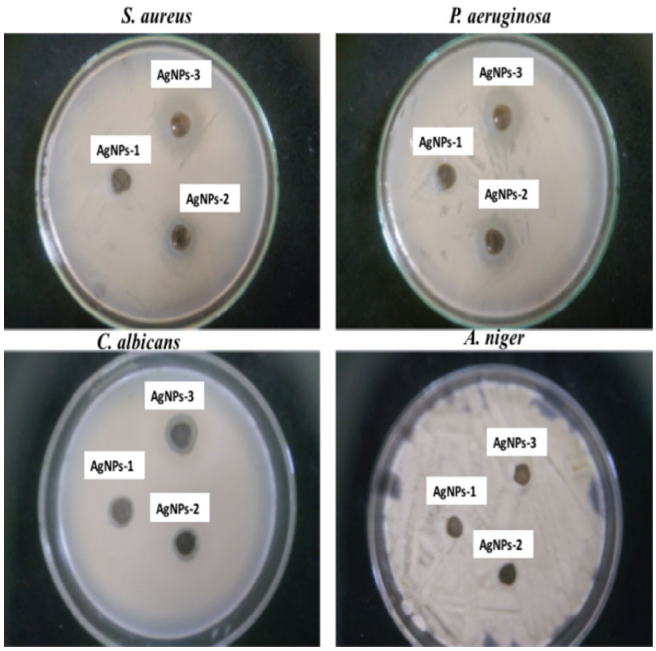

Fig. 10 Inhibition zone diameter of the as synthesized AgNPs in its solid state using different concentrations of $AgNO_3$. Where AgNPs-1 = 0.05 g $AgNO_3$/0.2 g Acacia and AgNP-2 = 0.10 $AgNO_3$/0.2 g Acacia and AgNPs-3 = 0.2 g $AgNO_3$/0.2 g Acacia

Sample No.	Clear Zone (mm)			
	S. aureus	*P. aeruginosa*	*C. albicans*	*A. niger*
AgNPs-1	14	13	18	0
AgNPs-2	22	21	21	0
AgNPs-3	24	24	23	0

clusters in the original highly concentrated solution as shown in Fig. 8E. The figures that marked with a, b, c, d, and e are taken for untreated and treated gauze cotton fabrics at high magnification.

Elemental Analysis of Treated Gauze Fabrics: (EDX)

Energy dispersive X-ray diffraction (EDX) analysis was used to confirm the presence of AgNPs. The gauze sample treated with AgNPs solution (0.06/100 mL H_2O) was selected for elemental analysis.

In Fig. 9, EDX spectrum of gauze cotton fabrics treated with AgNPs mediated via acacia is presented. An electron beam at (300 kV) excited samples and the elements Ag, C and O peaks were identified through. There are no significant impurities were found in the samples. Element mapping shows the homogeneity of the distribution of AgNPs on acacia surface.

Antibacterial Properties of AgNPs Mediated via Acacia (Powder Form)

AgNPs has been reported in the literature as a powerful antimicrobial agent against wide range of microorganisms. However, it is worthy to mention that it is recommended only for the topical applications in human. These restrictions might be attributed to the adverse effect on human health and interaction with cells [35, 36].

The antimicrobial efficacy of the as prepared AgNPs mediated via acacia gum was explored by measuring the zone of inhibition against; gram positive bacterium) *S. aureus*, gram negative bacterium) P. *aeruginosa*; *C. albicans* (yeast); and *A. niger* (fungus). Figure 10 shows the zone of inhibition of AgNPs powder sample was 14 mm, 24 mm and 22 mm for *S. aureus* for at sample AgNPs-1, AgNPs-2 and AgNPs-3, respectively. The zone of inhibition for *P. aeruginosa* was 13 mm, 24 mm and 21 mm for AgNPs-1, AgNPs-2 and AgNPs-3, respectively. Furthermore, the zone of inhibition for *C. albicans* was 18 mm, 23 mm and 21 mm for AgNPs-1, AgNPs-2 and AgNPs-3,

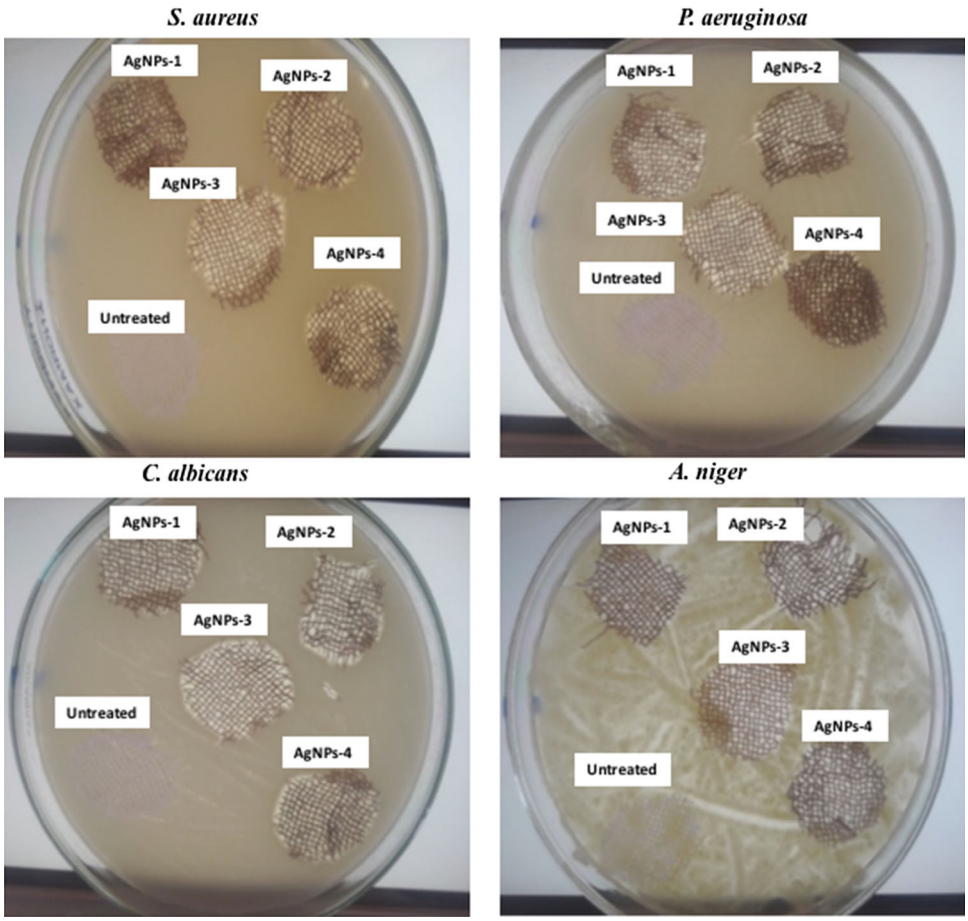

Fig. 11 Inhibition zone of the untreated and treated gauze fabric against *S. aureus*, gram (−ve) *P. aeruginosa* bacteria; *C. albicans* (yeast); and *A. Niger* (Fungus)

respectively. However, it was found that all samples have zero inhibition zone for *A. niger*.

Antibacterial for Gauze Fabric

Figure 11 shows the zone of inhibition of untreated and gauze fabrics treated with four different concentrations of AgNPs; (0.01 g/100 mL H_2O, 0.02 g/100 mL H_2O, 0.04 g/100 mL H_2O and 0.06 g/100 mL H_2O and nominated as AgNPs-1, AgNPs-2, AgNPs-3 and AgNPs-4 respectively. after against *Pseudomonas aeruginosa* culture. Nutrient agar was used as the media. Samples of cotton fabrics with various AgNPs concentrations were loaded into the well, which were made by using Cork borer method. The plates were incubated at 37 °C, for 24 h. Tetracycline was used as a standard. Figure 11 shows zero inhibition zone for untreated gauze cotton fabrics and shows a localized antibacterial activity of the treated samples. However, the bactericidal effect of AgNPs was localized underneath the gauze fabric instead of the whole dish. Therefore, further investigation is required and we resorted to the cell viable counting techniques.

Figure 12 shows the reduction percent in number of bacterial colonies of untreated and treated gauze fabrics in comparison to control *Pseudomonas aeruginosa* culture. Untreated gauze fabric has its marginal antimicrobial activity thus shows 12.69 reduction in CFU (%). However, sample of treated gauze with AgNPs-1, Ag^{-}NNPs-2, AgNPs-3 and AgNPs-4 for *Pseudomonas aeruginosa* reduction showed 57.94, 80.95, 95.23 and 100 reduction in CFU (%), respectively. These results confirm the antibacterial activity of gauze fabrics treated with AgNPs via bad-cure method.

Conclusion

A bioactive antimicrobial wound dressing was developed in which silver nanoparticles (AgNPs) were employed as an effective disinfectant agent. AgNPs was prepared via solid-state using acacia gum, which acted as both reductant and stabilizing agent. Acacia is a naturally occurring mixture of polysaccharides and glycoproteins and have been utilized in pharmaceuticals and food additives. The as synthesized AgNPs formed at different concentration of $AgNO_3$ were used to finish cotton gauze to produce a bioactive wound dressing. Several characterization techniques such as Uv–vis, TEM, DLS, zeta potential, SEM,

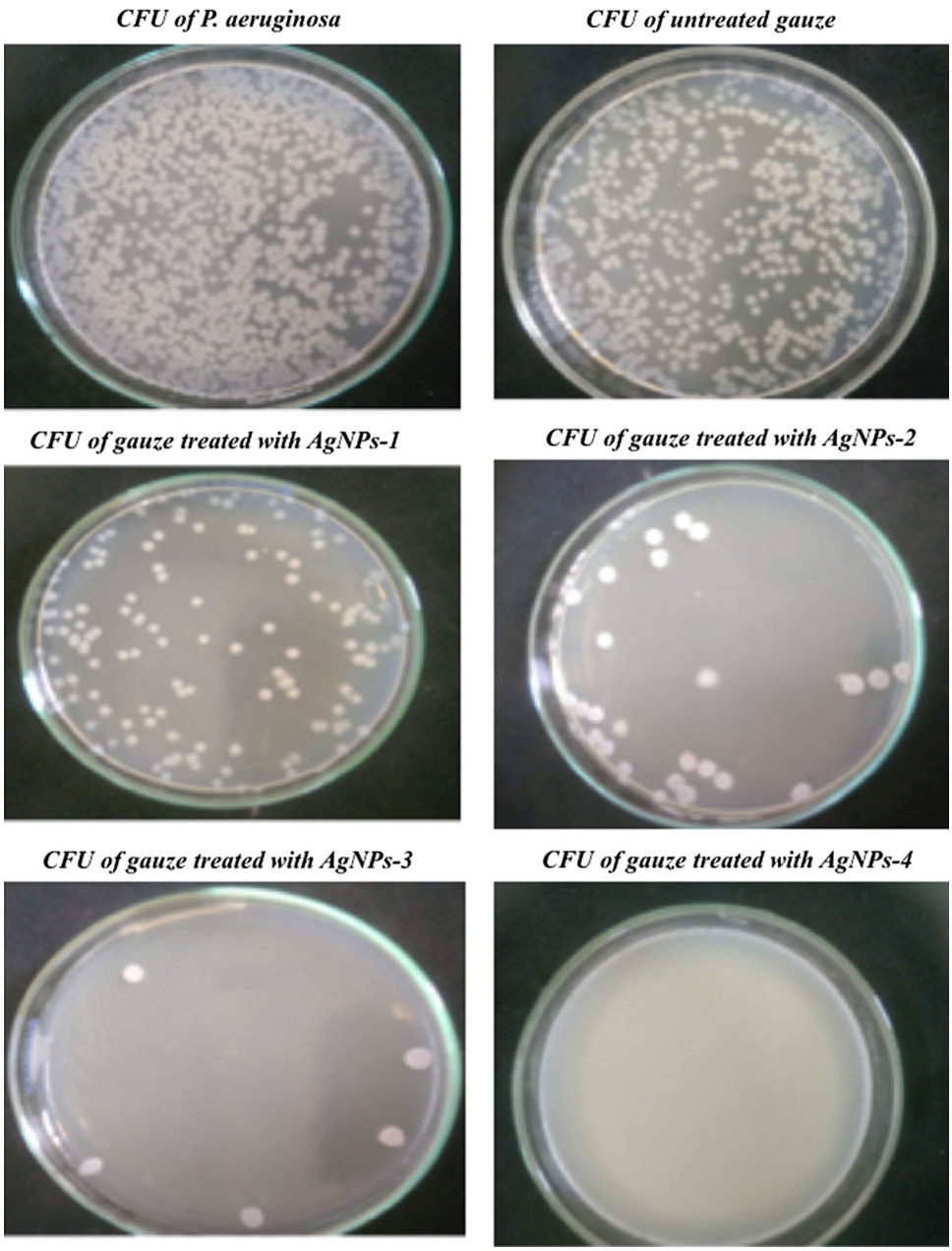

Fig. 12 Antibacterial evaluation of untreated and treated gauze fabric in comparison with *Pseudomonas aeruginosa* using CFU technique

EDX were utilized to investigate the properties of AgNPs. The obtained particles were in the range of 50 nm. The bioactivity, antimicrobial properties, of AgNPs treated gauze cotton fabrics against gram positive bacterium (*S. aureus*), gram negative bacterium (*P. aeruginosa*); yeast (*C. albicans*) and fungus (*A. niger*) was evaluated using the zone of inhibition. The inhibition zone of the as prepared AgNPs was found to be 24 mm against both types of bacteria, 23 mm against *C. albicans* and zero against *A. niger*. Additionally, the treated gauze cotton fabric did not create any inhibition zones on the agar plates, however, instead showed clear zone underneath the samples on the agar plate. This observation provides an evidence of non-release behavior of the treated gauze. Furthermore, the efficiency of the treated gauze fabric was quantitatively evaluated via measuring the reduction percent in number of bacterial colonies. The experiment was performed in comparison to control pseudomonas aeruginosa culture showed a reduction up to 100% reduction. The attained results endorse the activity of the prepared bioactive antimicrobial wound dressing.

References

1. D. Medhat, J. Hussein, M. E. El-Naggar, M. F. Attia, M. Anwar, Y. A. Latif, H. F. Booles, S. Morsy, A. R. Farrag, W. K. B. Khalil, and Z. El-Khayat (2017). *Biomed. Pharmacother.* **91**, 1006–1016.
2. J. Hussein, M. El-Banna, T. A. Razik, and M. E. El-Naggar (2018). *Int. J. Biol. Macromol.* **107**, (Pt A), 748–754.
3. A. I. El-Batal, N. M. Balabel, M. S. Attia, and G. S. El-Sayyad (2019). *J. Cluster Sci.* **30**, (4), 919–935. https://doi.org/10.1007/s10876-019-01550-7.
4. M. T. Rahimi, E. Ahmadpour, B. R. Esboei, A. Spotin, M. H. K. Koshki, A. Alizadeh, S. Honary, H. Barabadi, and M. A. Mohammadi (2015). *Int. J. Surg.* **19**, 128–133.
5. R. Balachandar, P. Gurumoorthy, N. Karmegam, H. Barabadi, R. Subbaiya, K. Anand, P. Boomi, and M. Saravanan (2019). *J. Clust. Sci*. **30**, 1481–1488. https://doi.org/10.1007/s10876-019-01591-y.
6. H. Barabadi, Z. Alizadeh, M. T. Rahimi, A. Barac, A. E. Maraolo, L. J. Robertson, A. Masjedi, F. Shahrivar, and E. Ahmadpour (2019). *Nanomed. Nanotechnol. Biol. Med.* **18**, 221–233.
7. T. K. Sau, A. L. Rogach, F. Jäckel, T. A. Klar, and J. Feldmann (2010). *Adv. Mater.* **22**, (16), 1805–1825.
8. Y. Xie, R. Ye, and H. Liu (2006). *Colloids Surf. A* **279**, (1–3), 175–178.
9. A. Hebeish, M. E. El-Naggar, S. Tawfik, S. Zaghloul, and S. Sharaf (2019). *Cellulose* **26**, (5), 3543–3555.
10. M. E. El-Naggar, T. I. Shaheen, M. Fouda, and A. Hebeish (2016). *Carbohydr. Polym.* **136**, 1128–1136.
11. M. Darroudi, A. K. Zak, M. Muhamad, N. Huang, and M. Hakimi (2012). *Mater. Lett.* **66**, (1), 117–120.
12. M. R. Karim, K. T. Lim, C. J. Lee, M. T. I. Bhuiyan, H. J. Kim, L. S. Park, and M. S. Lee (2007). *J. Polym. Sci. Part A* **45**, (24), 5741–5747.
13. D. Chen, X. Qiao, X. Qiu, J. Chen, and R. Jiang (2011). *J. Mater. Sci. Mater. Electron.* **22**, (1), 6–13.
14. G. R. Nasretdinova, R. R. Fazleeva, R. K. Mukhitova, I. R. Nizameev, M. K. Kadirov, A. Y. Ziganshina, and V. V. Yanilkin (2015). *Electrochem. Commun.* **50**, 69–72.
15. H. Barabadi, S. Honary, P. Ebrahimi, A. Alizadeh, F. Naghibi, and M. Saravanan (2019). *Inorgan. Nano-Metal Chem.* **49**, (2), 33–43.
16. H. Barabadi, B. Tajani, M. Moradi, K. D. Kamali, R. Meena, S. Honary, M. A. Mahjoub, and M. Saravanan (2019). *J. Cluster Sci.* **30**, 843–856.
17. R. Subbaiya, M. Saravanan, A. R. Priya, K. R. Shankar, M. Selvam, M. Ovais, R. Balajee, and H. Barabadi (2017). *IET Nanobiotechnol.* **11**, 965–972.
18. I. Virmani, C. Sasi, E. Priyadarshini, R. Kumar, S. K. Sharma, G. P. Singh, R. B. Pachwarya, R. Paulraj, H. Barabadi, M. Saravanan, and R. Meena (2019). *J. Clust. Sci.* https://doi.org/10.1007/s10876-019-01695-5.
19. A. M. Abdelgawad, M. E. El-Naggar, W. H. Eisa, and O. J. Rojas (2017). *J. Clean. Prod.* **144**, 501–510.
20. A. Hebeish, M. H. El-Rafie, A. M. Rabie, M. A. El-Sheikh, and M. E. El-Naggar (2014). *J. Appl. Polym. Sci.*. https://doi.org/10.1002/app.40170.
21. J. Hussein, M. E. El Naggar, Y. A. Latif, D. Medhat, M. El Bana, E. Refaat, and S. Morsy (2018). *Colloids Surf. B* **170**, 76–84.
22. D. Debnath, C. Kim, S. H. Kim, and K. E. Geckeler (2010). *Macromol. Rapid Commun.* **31**, (6), 549–553.
23. W. H. Eisa, A. M. Abdelgawad, and O. J. Rojas (2018). *ACS Sustain. Chem. Eng.* **6**, (3), 3974–3983.
24. A. Hebeish, T. I. Shaheen, and M. E. El-Naggar (2016). *Int. J. Biol. Macromol.* **87**, 70–76.
25. N. Maffulli, P. Renström, and W. B. Leadbetter *Tendon injuries* (Springer, Berlin, 2005).
26. H. Ueno, H. Yamada, I. Tanaka, N. Kaba, M. Matsuura, M. Okumura, T. Kadosawa, and T. Fujinaga (1999). *Biomaterials* **20**, (15), 1407–1414.
27. A. C. de O. Gonzalez, T. F. Costa, Z. de A. Andrade, and A. R. A. P. Medrado (2016). *An. Bras. Dermatol.* **91**, 614–620. https://doi.org/10.1590/abd1806-4841.20164741.
28. S. Gupta, A. Agarwal, N. K. Gupta, G. Saraogi, H. Agrawal, and G. P. Agrawal (2013). *Drug Dev. Ind. Pharm.* **39**, 1866–1873.
29. L. I. F. Moura, A. M. A. Dias, E. Carvalho, and H. C. de Sousa (2013). *Acta Biomater.* **9**, 7093–7114.
30. T. Abdelrahman and H. Newton (2011). *Surgery* **29**, (10), 491–495.
31. E. A. Kamoun, E. -R. S. Kenawy, and X. Chen (2017). *J. Adv. Res*. **8**, 217–233.
32. A. I. Mekkawy, M. A. El-Mokhtar, S. M. El-Shanawany, and E. H. Ibrahim (2016). *Br. J. Pharm. Res.* **14**, 1–19.
33. S. Honary, H. Barabadi, E. Gharaei-Fathabad, and F. Naghibi (2013). *Trop. J. Pharm. Res.* **12**, (1), 11.
34. A. Hebeish, M. El-Rafie, M. El-Sheikh, and M. E. El-Naggar (2014). *J. Inorgan. Organomet. Polym. Mater.* **24**, (3), 515–524.
35. H. Barabadi, M. Najafi, H. Samadian, A. Azarnezhad, H. Vahidi, M. A. Mahjoub, M. Koohiyan, and A. Ahmadi (2019). *Medicina* **55**, (8), 439.
36. K. Mortezaee, M. Najafi, H. Samadian, H. Barabadi, A. Azarnezhad, and A. Ahmadi (2019). *Chem. Biol. Interact.* **312**, 108814.